Int. J. Multiphase Flow Vol. 14, No. 4, pp. 507–517, 1988
Printed in Great Britain.

0301-9322/88 $3.00 + 0.00

THE EFFECT OF THREE CLOSURES ON CRITICAL CONDITIONS IN TWO-PHASE FLOW WITH UNEQUAL PHASE VELOCITIES

Z. BILICKI,† J. KESTIN and M. M. PRATT
Division of Engineering, Brown University, Providence, RI 02912, U.S.A.

(*Received* 11 *September* 1987; *in revised form* 26 *December* 1987)

Abstract—The paper develops an analytic approach to assess the effect of three closure conditions on the critical-flow state in two-phase flow. The approach is based on the geometrical–topological analysis of dynamical systems.

The details of the analysis are developed in relation to a "general slip" model which is completed by three closure conditions: homogeneous flow, Bankoff's hypothesis and the drift–flux model. For the sake of simplicity, the study is restricted to adiabatic flows and thermodynamic equilibrium. These make it possible to reduce the model to a single quasi-linear differential equation and to parametrize the problem with respect to the mass-flow rate $\dot{m}$ and the total stagnation enthalpy $\mathbf{h}$. The phase space is thus reduced to the P, z diagram.

Detailed results are given for the flow of water/steam through a convergent–divergent nozzle discharging from a stagnation reservoir. All three closures lead to the same topological structure of the "potrait" of solutions in the phase space which incorporates a saddle point.

The numerical results are summarized in table 1. This shows that the location of the critical cross-section (saddle point) is essentially unaffected by the closure chosen for the model; it is situated very close to the throat and downstream from it. The most significant critical-flow characteristics, such as mass-flow rate, critical pressure, critical velocity, critical void fraction and critical slip velocity differ markedly from those predicted by the homogeneous-flow assumption when the effects of slip are included. The differences between the two closures with the slip are significant but much smaller than between either of them and the no-slip model.

All models calculate a very large increase in the void fraction as the critical state near the throat is approached. This is interpreted to mean that none of the three closures should be used to analyze critical flows, because their validity has been tested only for much lower values of void fraction.

The critical velocity is a sole function of the local thermodynamic state. The two slip closures lead to considerable differences in this relationship when compared with the sound velocity under homogeneous-flow conditions.

Key Words: two-phase flow, critical flow, slip model, two-phase flow modelling, closures for two-phase flow models, convergent–divergent nozzle, drift–flux closure, Bankoff's closure

1. INTRODUCTION

The purpose of this paper is to develop a predominantly analytic approach to the assessment of the effects of three closure conditions on the critical-flow state in two-phase flow. At the point where algebraic complexity makes it unavoidable, numerical results are generated by computer. Such an approach is more efficient than one based on a large number of computer print-outs, apart from leading to a clearer grasp of the underlying physics. The qualitative analysis employed in this paper can be exploited to discriminate between closure conditions regarding their quality and, in the light of reliable experimental data, on critical flow; its use greatly facilitates the task of predicting the occurrence of critical-flow conditions in terms of a preferred mathematical model, as shown by Bilicki *et al.* (1987).

The current state of the art provides no generally accepted set of equations which could serve as a basis for a preferred model. This conviction has been confirmed and reinforced by two recent workshops (see Hewitt *et al.* 1987, 1988). To illustrate the method in this paper, we have chosen a relatively simple, two-velocity model based on the usual three conservation laws. The model is spatially one-dimensional, operates with time-averaged properties, and integral averages taken over a cross-section. The present "general slip" model is so constructed that specialization to three closure conditions can be easily accomplished. The three closure conditions selected for study are: homogeneous flow, Bankoff's (1960) proposal for slip and the drift–flux model (Zuber & Findlay 1965). A similar model was used by Lyczkowski (1978) and others (Ishii 1977; Lahey & Moody

†Permanent address: Institute of Fluid Flow Machinery, Polish Academy of Sciences, Gdansk, Poland.

1984). Some well-known results for the homogeneous model are introduced as a reference, but the results for unequal velocities of the phases are new. Although the model admits the existence of unequal local velocities of the two phases, it is limited to a uniform pressure and thermodynamic equilibrium in a cross-section.† For the sake of simplicity only adiabatic flows are analyzed.

2. THE MODEL EQUATIONS

Applying the mean-value theorem to integral forms (e.g. Delhaye 1981), we are led to the following conservation laws:

$$\frac{\mathrm{d}}{\mathrm{d}z}(A\rho w) = 0, \tag{1a}$$

$$A\frac{\mathrm{d}P}{\mathrm{d}z} + \frac{\mathrm{d}}{\mathrm{d}z}[A\rho(w^2 + xyu^2)] = -2(\pi A)^{1/2}\tau, \tag{1b}$$

$$\frac{\mathrm{d}}{\mathrm{d}z}\left[\!\left[A\rho\{[h + \tfrac{1}{2}(w^2 + xyu^2)]w + xy[h_\mathrm{G} - h_\mathrm{L} + uw - \tfrac{1}{2}(y - x)u^2]u\}\right]\!\right] = 0. \tag{1c}$$

Here, A denotes the area of the cross-section, ρ is the density, w the velocity, P the pressure and τ the shearing stress. All properties represent cross-sectional averages of time-averaged quantities. The phase composition is measured by the "static" dryness fraction

$$x = \frac{v - v_\mathrm{L}}{v_\mathrm{G} - v_\mathrm{L}} \qquad \left(v = \frac{1}{\rho};\quad 1 - x = y\right), \tag{2}$$

where the subscripts G and L, respectively, refer to the vapor and liquid. This quantity is related to the void fraction by

$$\alpha(x, P) = \frac{xv_\mathrm{G}}{v}. \tag{3a}$$

The equations include the slip velocity $u = w_\mathrm{G} - w_\mathrm{L}$ and the mixture enthalpy

$$h = \frac{[\alpha\rho_\mathrm{G}h_\mathrm{G} + (1 - \alpha)\rho_\mathrm{L}h_\mathrm{L}]}{\rho}. \tag{3b}$$

The preceding model constitutes a system of three ordinary, coupled, nonlinear differential equations for the four unknown functions of longitudinal distance

$$P(z), v(z), w(z) \quad \text{and} \quad u(z). \tag{4}$$

The fourth equation is provided by the closure condition which we assume in the form of an explicit expression in the slip velocity u. As already stated, we consider three examples for future comparison:

(a) The homogeneous model, with

$$u = 0. \tag{5}$$

(b) Bankoff's (1960) expression for the slip ratio

$$S = \frac{w_\mathrm{G}}{w_\mathrm{L}} = \frac{1 - \alpha}{\mathrm{K} - \alpha}, \tag{6a}$$

where K is a constant ranging from 0.7 to 0.9 In terms of our variables, this hypothesis is equivalent to

$$u = \frac{1 - \mathrm{K}}{\mathrm{K} - \alpha + x(1 - \mathrm{K})}w, \tag{6b}$$

†It is not suggested that this is necessarily a justified assumption; it is made for concreteness. Nonequilibrium flows can be treated with the aid of the same formalism.

where $\alpha(x, P)$ has the form given in [3a]. The usefulness of this closure is limited to low values of void fraction.† We note that Bankoff's model reduces itself to the homogeneous model for $K = 1$.

(c) The drift–flux model postulates that

$$w_G = V_{G_j} + C_0 j, \tag{7a}$$

where

$$j = \alpha w_G + (1 - \alpha) w_L \tag{7b}$$

is the velocity of the volumetric center of the mixture. V_{Gj} is the difference between the average velocity of the gaseous phase and the velocity of the volumetric center. The quantity C_0 is known as the distribution parameter. Ishii (1977) and Ishii & Zuber (1979) have given a number of correlations for V_{Gj} and C_0, both of which depend on the flow pattern and differ from diagram to diagram, albeit within the comparatively narrow limits of 1.0–1.5 for C_0 and 0–1 m/s for V_{Gj}. The slight departures from linearity in the w_G vs j diagram are ignored.

We express the slip velocity in terms of the drift–flux model parameters and obtain, after a somewhat lengthy calculation, the relation

$$u = \frac{V_{Gj} + (C_0 - 1)w}{y\left[1 - C_0\left(1 - \frac{v_L}{v}\right)\right]}. \tag{7c}$$

3. GENERAL FEATURES OF THE ANALYTIC METHOD

The analytic method to be applied to the model consisting of [1a–c], augmented by the closure conditions [5], [6b] and [7c], taken in turn, has been presented in detail by Bilicki *et al.* (1987). The theory contained therein makes it possible to determine the "portrait" of the ensemble of solutions of the class of models whose canonical form is

$$\mathbf{A}(\boldsymbol{\sigma})\frac{d\boldsymbol{\sigma}}{dz} = \mathbf{B}(\boldsymbol{\sigma}, z), \tag{8}$$

of which the present one is a member. In our case, the vector $\boldsymbol{\sigma}$ has the $n = 3$ components P, v and w mentioned in [4]. The $n \times n$ matrix $\mathbf{A}$ and the n-vector $\mathbf{B}$ are specified by each model. Several detailed applications have been given by Bouré (1986, 1987a, b).

In the present case, the representation can be simplified considerably if it is noticed that [1a] and [1c] can be integrated explicitly, thus providing the following two "constants of the motion", the mass-flow rate

$$\dot{m} = A\rho w \tag{9a}$$

and the stagnation enthalpy

$$\mathbf{h} = h + \tfrac{1}{2}w^2 + \tfrac{1}{2}xyu^2 + xy[h_G - h_L + uw + \tfrac{1}{2}(y - x)u^2]\frac{u}{w}. \tag{9b}$$

By a process of tedious elimination, the set of equations [1a–c] can be reduced to the following, single, nonlinear ordinary differential equation

$$\frac{dP}{dz} = \frac{\mathbf{b}(P, z;\ \dot{m}, \mathbf{h})}{\mathbf{a}(P, z;\ \dot{m}, \mathbf{h})}. \tag{10}$$

An early and more direct analysis of an equation of the same type which occurs in single-phase flow was given by Kestin & Zaremba (1952). However, in this paper, we prefer to cast our treatment in the same terms as those used by Bilicki *et al.* (1987) in the most general case.

†These must satisfy the condition $\alpha \ll K$, because when α approaches the value of K (of order 0.9), the slip ratio assumes unrealistic values.

Explicit expressions for the functions **a** (equivalent to **A**) and **b** (equivalent to **B**) are listed in the appendix. The terms are so arranged that the three closures can be inserted into them explicitly. In the case of the homogeneous model with $u = 0$ we obtain the very easy-to-handle forms†

$$\mathbf{a} = 1 + w^2 \frac{v\,\partial_h v + \partial_P v}{v^2} \qquad [11a]$$

and

$$\mathbf{b} = \rho \left[w^2 \frac{R'}{R} - \frac{f w^2}{R} \left(1 + w^2 \frac{\partial_h v}{v} \right) \right]. \qquad [11b]$$

In the case of the other two closures, we must supplement the analysis with numerical calculations.

4. CRITICAL FLOW

The autonomous form of [10] is

$$\frac{\mathrm{d}z}{\mathrm{d}\xi} = \mathbf{a}(P, z;\ \dot{m}, \mathbf{h}), \qquad [11c]$$

$$\frac{\mathrm{d}P}{\mathrm{d}\xi} = \mathbf{b}(P, z;\ \dot{m}, \mathbf{h}), \qquad [11d]$$

where ξ is a dummy parameter. The phase space of our system reduces itself to the two-dimensional P, z diagram. The values of **a** and **b** at any point determine the direction of the tangent vector $\mathbf{V}(P, z)$, where $V_z = \mathbf{a}$ and $V_P = \mathbf{b}$. The "portrait" of the ensemble of solutions is clearly described by the vector field **V**. In particular, singular points P^*, z^* are described by

$$\mathbf{a} = \mathbf{b} = 0. \qquad [11e]$$

The topological character of each singular point is determined by the eigenvalues of the linearized version of [11c,d].

In order to attain critical-flow conditions, it is necessary to satisfy $\mathbf{a} = 0$ at the end of the channel or to create a saddle point with conditions $\mathbf{a} = \mathbf{b} = 0$ inside the channel. Many worked examples show that such a condition can be produced near a throat. Nodal points (e.g. Kestin & Zaremba 1954) are sufficiently rare in the absence of strong centrifugal forces to be safely ignored here.

"Portraits" involving a saddle point near a throat and a locus of turning points have been discussed in several earlier studies (Bilicki *et al.* 1987). The resulting pattern is quite familiar from elementary gas dynamics, except for the fact that now the location of the various characteristic points and curves follows from more complex calculations. The contribution of this analysis is to show its relevance under much more general circumstances than those habitually assumed in gas dynamics.

In all succeeding examples, the character of the singular points has been ascertained with reference to the linearized matrix, mentioned earlier and described by Bilicki *et al.* (1987).

In the remaining part of this paper we examine the effect of the three closure conditions when **h** and the pressure P_0 are specified at the upstream reservoir together with the requirement that the flow trajectory should pass through the saddle point. The values of **h** and P_0 place the stagnation state as well as the state at the entrance ($z_1 = 0$) in the liquid region. Flashing occurs between $z = 0$ and the throat.

5. NUMERICAL RESULTS

The following numerical values have been assumed in the calculations:

$$f = \frac{\tau}{\frac{1}{2}\rho w^2} = 0.008 \qquad C_0 = 1.2$$

$$\mathrm{K} = 0.89 \qquad \mathbf{h} = 762.2\ \mathrm{kJ/kg}$$

$$V_{Gj} = 0.4\ \mathrm{m/s} \qquad P_1 = 10\ \mathrm{b}.$$

The nozzle profile is the same as that studied by Bilicki *et al.* (1987).

†We use the compact notation for partial derivatives: $\partial_h v \equiv (\partial v/\partial h)_P$ etc.

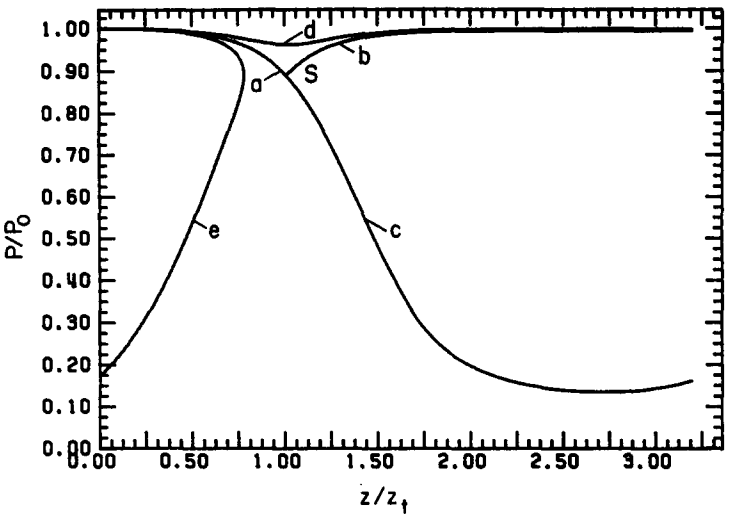

Figure 1a. P, z diagram: homogeneous-flow model. S—saddle point; a–b–c—critical flow $\dot{m}^*$; d—reduced flow rate $\dot{m} = 0.9\dot{m}^*$ (physically attainable); e—increased flow rate $\dot{m} = 1.1\dot{m}$ (physically attainable only in truncated nozzle).

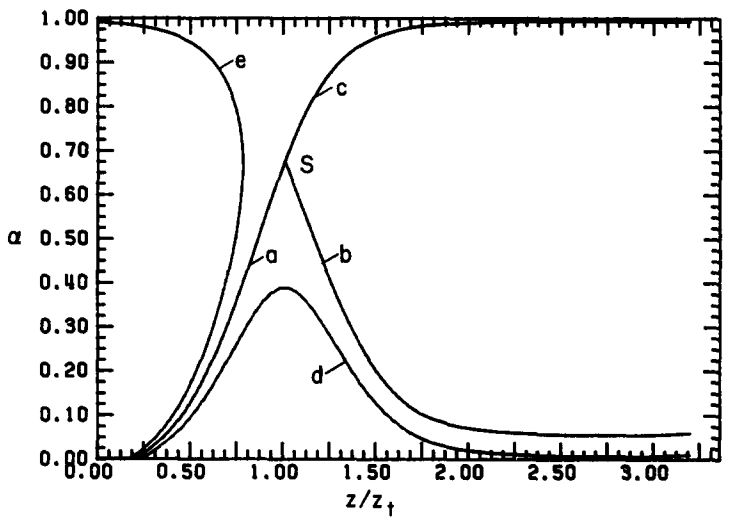

Figure 1b. α, z diagram: homogeneous-flow model. S—saddle point; a–b–c—critical flow $\dot{m}^*$; d—reduced flow rate $\dot{m} = 0.9\dot{m}^*$ (physically attainable); e—increased flow rate $\dot{m} = 1.1\dot{m}$ (physically attainable only in truncated nozzle).

The results that follow were obtained by inverse integrations starting with the saddle point S whose location must satisfy $\mathbf{a} = \mathbf{b} = 0$. This integration is iterated by computer until the required stagnation conditions are satisfied. Such a procedure is more efficient than trying to locate the saddle point by forward integration since trajectories diverge in the neighborhood of the saddle point.

The diagrams in figures 1a, 2a and 3a give an idea of the "portraits" of solutions for the three closure conditions. Each diagram traces the trajectories a, b, c which pass through the critical cross-section S while starting in the subcritical region with the above inlet conditions. Along each one of them, the critical mass-flow rate, $\dot{m}^*$, has a value which is induced by the respective closure. In addition, each diagram shows a trajectory d with $\dot{m} = 0.9\dot{m}^*$ (pressure minimum) and one, e, with $\dot{m} = 1.1\dot{m}^*$ incorporating a turning point. No trajectory of the family e can be produced in practice other than by truncating the nozzle at the turning point. Corresponding diagrams in the α, z-plane are displaced in figures 1b, 2b and 3b.

The data in table 1 represent the characteristic values of the three critical flows under discussion. The following conclusions can be drawn:

1. The location of the critical point is hardly affected by the pressure or the slip; in each case $z^*/z_t \approx 1.01$. This insensitivity of the location of the critical cross-section to varying condition has been observed by us before.
2. The critical pressure ratio (0.890, 0.540, 0.555) is strongly affected by slip, but the effects of the two different slip closures are not much different. The drift–flux model exhibited a higher critical slip velocity and a higher critical slip ratio than Bankoff's model, but it would be premature to assume that such a tendency is general.
3. The critical mass-flow rate does not seem to be a monotone function of the critical velocity.

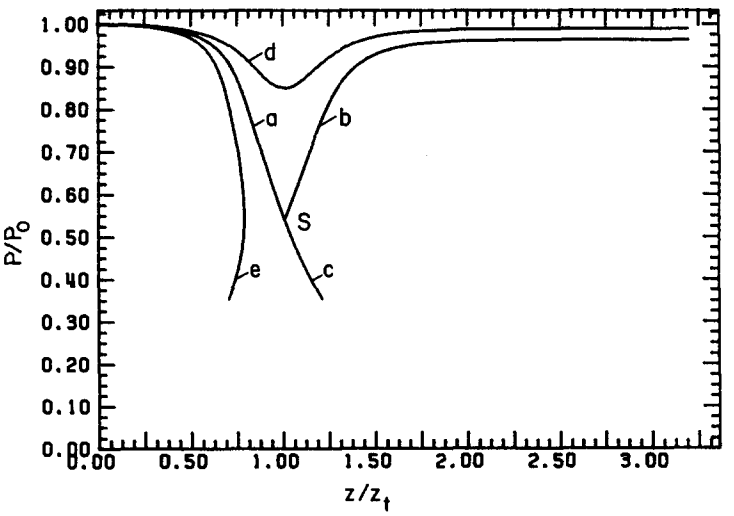

Figure 2a. P, z diagram: slip model, Bankoff closure. S—saddle point; a–b–c—critical flow $\dot{m}^*$; d—reduced flow rate $\dot{m} = 0.9\dot{m}^*$ (physically attainable); e—increased flow rate $\dot{m} = 1.1\dot{m}$ (physically attainable only in truncated nozzle).

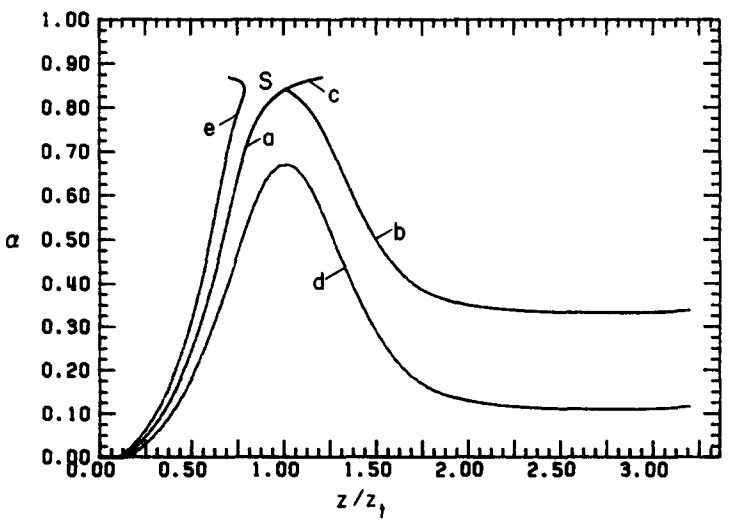

Figure 2b. α, z diagram: slip model, Bankoff closure. S—saddle point; a–b–c—critical flow $\dot{m}^*$; d—reduced flow rate $\dot{m} = 0.9\dot{m}^*$ (physically attainable); e—increased flow rate $\dot{m} = 1.1\dot{m}$ (physically attainable only in truncated nozzle).

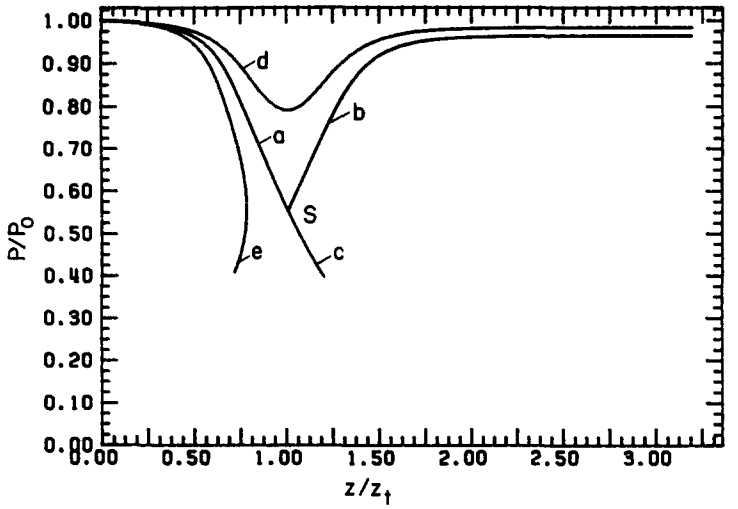

Figure 3a. P, z diagram: slip model, drift-flux closure. S—saddle point; a–b–c—critical flow $\dot{m}^*$; d—reduced flow rate $\dot{m} = 0.9\dot{m}^*$ (physically attainable); e—increased flow rate $\dot{m} = 1.1\dot{m}$ (physically attainable only in truncated nozzle).

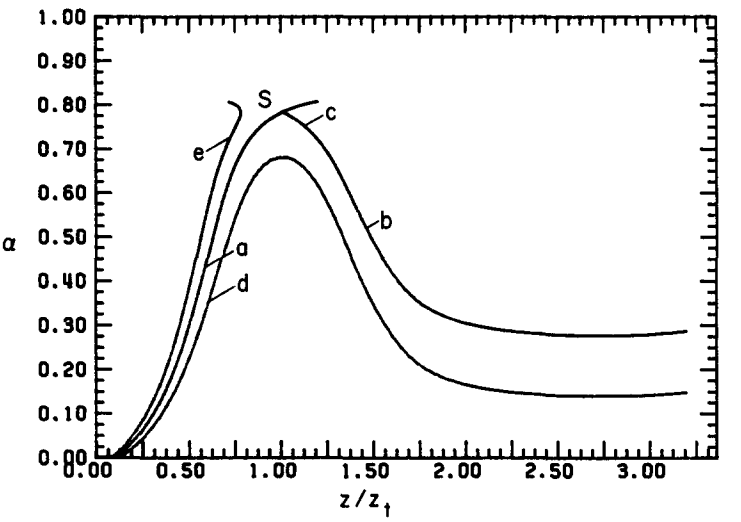

Figure 3b. α, z diagram: slip model, drift-flux closure. S—saddle point; a–b–c—critical flow $\dot{m}^*$; d—reduced flow rate $\dot{m} = 0.9\dot{m}^*$ (physically attainable); e—increased flow rate $\dot{m} = 1.1\dot{m}$ (physically attainable only in truncated nozzle).

Table 1. Critical parameters for the channel of figure 2. Effect of three closures: $\mathbf{h} = 762.2$ kJ/kg, $P_0 = 10$ b, $z_t = 0.25$ m

		Model		
		(a) Homogeneous	(b) Bankoff	(c) Drift-flux
Inlet velocity, m/s	w_1	1.82	2.43	2.80
Critical mass-flow rate, kg/s	$\dot{m}$	50.6	67.8	78.1
Location of critical cross-section, m	z^*	0.253	0.252	0.252
Critical pressure, b	P^*	8.90	5.40	5.55
Critical velocity, m/s	w^*	22.0	58.5	49.7
Critical void fraction	α^*	0.670	0.841	0.783
Critical slope, b/m	$\left(\frac{dP}{dz}\right)^*$	$\begin{cases} -18 \\ +19 \end{cases}$	$\begin{matrix} -43 \\ +45 \end{matrix}$	$\begin{matrix} -35 \\ +36 \end{matrix}$
Critical slip velocity, m/s	u^*	0	127	164
Critical slip ratio	S^*	1	3.3	4.4

4. Bankoff's and the drift–flux models show a marked similarity. This might have been expected if it is noticed that for the drift–flux model the slip ratio satisfies

$$S = \frac{1-\alpha}{\dfrac{j}{(V_{Gj}+C_0 j)} - \alpha}. \qquad [12]$$

6. CRITICAL VELOCITY

The general theory of mathematical models of the type of [8] shows that its homogeneous form determines the critical velocity w^* which is thus a clear function of the local thermodynamic parameters, regardless of the form of **B** or **b**, that is of the shape of the channel and the mass-flow rate. However, the closure conditions affect the form of **a** and so also the local critical relationships.

To see it clearly in the present case, we note that in the previous section we integrated [10] to determine the trajectory $P(z)$, treating **a** and **b** as functions of P and z† with $\dot{m}$ and **h** playing the role of parameters. But an examination of the terms of **a** in the appendix shows that we can treat **a** as a function of P, v and w. The solution of the equation $\mathbf{a} = 0$ then yields the critical velocity w^* as a function of the local thermodynamic variables P and v independently of the channel geometry or the mass-flow rate.

It can be seen that the three closure conditions are each linear functions of w. As a result, the condition $\mathbf{a} = 0$ leads to a quartic in w^*. In the case of the homogeneous model, as indicated in [11a], it degenerates to the expected result that

$$w^{*2} = -\frac{v^2}{v\,\partial_h v + \partial_P v}, \qquad [13a]$$

easily proved to be equivalent to

$$w^{*2} = \partial_\rho P \text{ at constant entropy.} \qquad [13b]$$

The preceding consideration shows that the choking velocity w^*, associated with the speed of sound in gas dynamics, is a unique function of the local thermodynamic state in all three cases, albeit of a different form in each. Since the coefficients in the quartic equation depend on the assumed closure conditions, it becomes clear that the choking velocity depends on the mechanisms which produce slip.

The condition $\mathbf{a} = 0$ was solved for each of the three closures and the results are shown in figures 4a and 4b. In figure 4a, P is the independent variable and the stagnation enthalpy $\mathbf{h} = 762.2$ kJ/kg. Specification of **h** allows us to determine the specific volume v from [9b] as a function of P and w. Thus the calculation of w^* reduces itself to solving

$$\mathbf{a}\{P, w^*, v(P, w^*)\} = 0 \qquad [14]$$

for w^* at each value of P.

The values of void fraction are calculated from v at the given pressure with the aid of [2] and [3]. In figure 4b the void fraction itself is chosen as the independent variable, the pressure having been fixed at $P^* = 10$ b.

Examination of the two plots in figures 4a and 4b shows, as expected, that the critical speed w^* predicted by the two slip models approaches that implied in the homogeneous-flow model for small values of void fraction α. Further, both plots show that the critical speed passes through a maximum in α when slip is present and differs considerably from that implied in homogenous flow at higher values of α.

The plot in figure 4a can be interpreted to explain that the higher critical mass-flow rates predicted by the models with slip are due to sharply lower values of the critical void fraction compared with the homogeneous-model results and are not due to higher critical velocities.

†The coordinate z appears explicitly in the function **a** through the substitution $w = \dot{m}/\rho A(z)$.

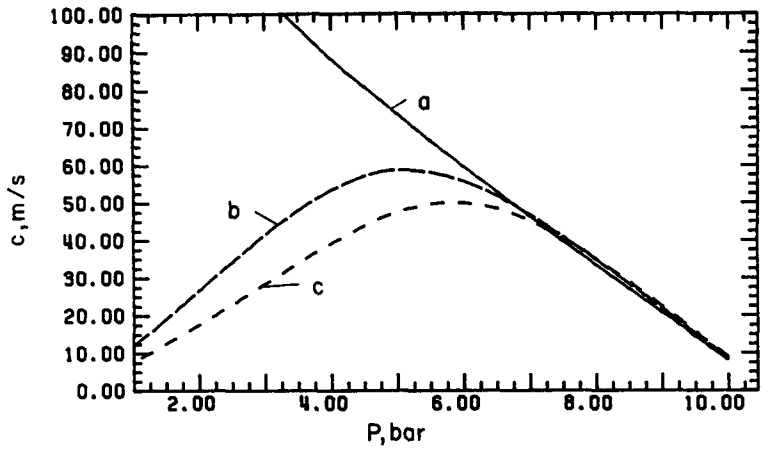

Figure 4a. Critical velocity for the three models as a function of local pressure: (a) homogeneous model; (b) Bankoff's model; (c) drift–flux model, $\mathbf{h} = 762.2$ kJ/kg.

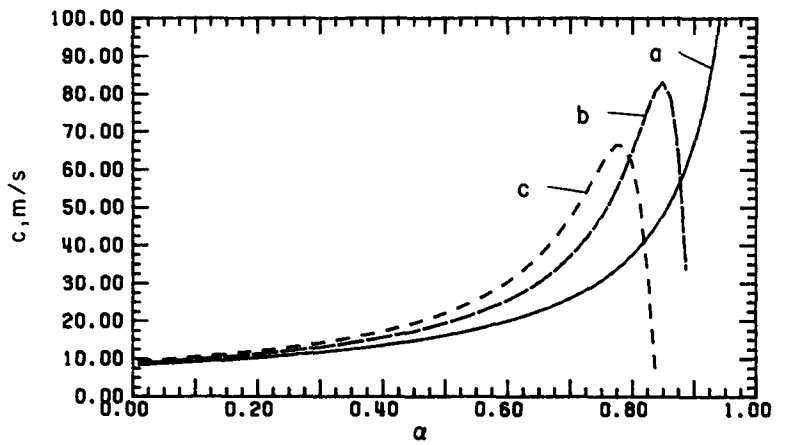

Figure 4b. Critical velocity for the three models as a function of local void fraction with $P^* = 10$ b: (a) homogeneous model; (b) Bankoff's model; (c) drift–flux model, $\mathbf{h} = 762.2$ kJ/kg.

7. INTERPRETATION

The use of the no-slip, homogeneous-flow model is the result of a natural desire for simplicity and for the convenience of being able to fall back on the results of elementary gas dynamics; its utility is admittedly limited, except as a convenient vehicle for comparisons. The other two closures discussed here have been developed specifically to allow for the existence of slip in actual flows; their utility has been proven for dispersed flows of relatively low void fractions. It has been pointed out in sections 2 and 5 that both slip closures lead to obviously unrealistically high slip velocities when the void fraction reaches values of the order of 0.8. The results adduced in section 5 emphasize a severe limitation of their applicability under near-critical conditions. This is a compelling conclusion that we must draw from table 1 and figures 1b, 2b and 3b. In all three cases the void fraction at inlet starts with $\alpha_1 = 0$ and passes through very low values, and yet the "predicted" critical value near the throat is of order $\alpha^* \approx 0.7$–0.8 in all three cases. Additional calculations, omitted here for lack of space, confirm the otherwise known fact that the dryness fraction increases fast as critical conditions are approached because of the high rate of evaporation which accompanies fast rates of pressure drops. It follows that all three closures break down somewhere between the inlet and the throat and neither can be recommended for the analysis of flows through channels with varying cross-sectional areas and, particularly, through convergent–divergent nozzles.

The same diagrams forcefully suggest, as intimated in the introduction, that experimental results on nozzles can be very useful in the assessment of the validity of closures. At the present time there are not enough reliable experimental data on such flows in the published literature. A program of this kind would materially contribute to the advancement of the discussion on the "closure issue" so ably illuminated by J. Bouré (1986, 1987a, b).

In addition to providing indications on how to contribute to the resolution of the "closure issue", the analysis of sections 4 and 5 draws attention to the fact that normally employed closures are most probably inadequate to cover flows whose representative points in phase space fall between the subcritical and supercritical branches downstream from the saddle point (if and when it must be expected).

Acknowledgements—The authors wish to acknowledge the financial support received from the Office of Energy Engineering Research of the U.S. Department of Energy under Grant DE-FG02-87ER-13687. Special thanks are due to Dr O. P. Manley, the Project Manager, for his continuous interest and encouragement.

REFERENCES

BANKOFF, S. G. 1960 A variable density single-fluid model for two-phase flow with particular reference to steam–water flow. *J. Heat Transfer, Trans. ASME* **82,** 265–272.

BILICKI, Z., DAFERMOS, C., KESTIN, J., MAJDA, G. & ZENG, D.-L. 1987 Trajectories and singular points in steady-state models of two-phase flows. *Int. J. Multiphase Flow* **13,** 511–533.

BOURÉ, J. A. 1986 Two-phase flow models: "The closure issue". Lecture notes for *Eur. Two-phase Gp Mtg*, Munich, 9–13 June.

BOURÉ, J. A. 1987a Properties and modeling of kinematic and pressure waves in two-phase flows. Lecture notes for *ICHMT Int. Semin. on Transient Phenomena in Multiphase Flow*, Dubrovnik, 24–30 May.

BOURÉ, J. A. 1987b Two-phase flow models: "The closure issue". In *Multiphase Science and Technology*, Vol. 3 (Edited by HEWITT, G. F., DELHAYE, J. M. & ZUBER, N.), pp. 3–30. Hemisphere, Washington, D.C.

DELHAYE, J. M. 1981 Local instantaneous equations. In *Industrial Design and Nuclear Engineering* (Edited by DELHAYE, J. M., GIOT, M. & RIETHMULLER, M. L.), pp. 95–101. Hemisphere, Washington, D.C.

HEWITT, G. G., DELHAYE, J. M. & ZUBER, N. (Eds) 1987 *Multiphase Science and Technology*, Vol. 3. Hemisphere, Washington, D.C.

HEWITT, G. F., DELHAYE, J. M. & ZUBER, N. (Eds) 1988 *Multiphase Science and Technology*, Vol. 4. Hemisphere, Washington, D.C. To be published.

ISHII, M. 1977 One-dimensional drift–flux model and constitutive equations for relative motion between phases in various two-phase flow regimes. Argonne National Lab. Report ANL-77-47.

ISHII, M. & ZUBER, N. 1979 Drag coefficient and relative velocity in bubbly, droplet and particulate flows. *AIChE Jl* **25,** 843–855.

KESTIN, J. & ZAREMBA, S. K. 1952 Geometrical methods in the analysis of ordinary differential equations. *Appl. scient. Res.* **B3,** 149–189.

KESTIN, J. & ZAREMBA, S. K. 1954 Adiabatic one-dimensional flow of a perfect gas through a rotating tube of uniform cross-section. *Aeronaut. Q.* **4,** 373–399.

LAHEY, R. T. JR & MOODY, F. M. 1984 *The Thermal Hydraulics of a Boiling Water Nuclear Reactor*. American Nuclear Soc., Hinsdale, Ill.

LYCZKOWSKI, R. W. 1978 Theoretical bases of the drift–flux field equations and vapor drift velocity. *Proc. 6th Int. Heat Transfer Conf.*, Toronto, pp. 339–344.

ZUBER, N. & FINDLAY, J. A. 1965 Average volumetric concentration in two-phase flow systems. *J. Heat Transfer, Trans. ASME* **87,** 453–468.

See Opposite for the Appendix

APPENDIX

Explicit Expressions for the Functions $\mathbf{a}(P, z;\ \dot{m}, \mathbf{h})$ *and* $\mathbf{b}(P, z;\ \dot{m}, \mathbf{h})$ *from [10]*

A circular cross-section with $A(z) = \pi[R(z)]^2$ and $C = 2\pi R$ has been assumed; $R' \equiv \mathrm{d}R/\mathrm{d}z$. The shearing stress is assumed as $\tau = 1/2 f\rho w^2$.

The functions **a** and **b** in [10] follow from the reduction of the three mixture conservation laws to a single equation by using the mass conservation and energy conservation integrals. The derivation is tedious, so only the result is stated here:

$$\mathbf{a} = a_1 y_1 - y_2 a_2, \tag{A.1}$$

$$\mathbf{b} = b_1 y_1 - y_2 b_2, \tag{A.2}$$

$$a_1 = 1 + \rho u^2\, \partial_P(xy) + 2\rho xyu\, \partial_P u, \tag{A.3}$$

$$a_2 = -\partial_P v + \frac{\partial_h v}{w}\left\{\tfrac{3}{2}u^2 w\, \partial_p(xy) + u\, \partial_p[xy(h_G - h_L)] + \tfrac{1}{2}u^3\, \partial_P[xy(y-x)] + a_3\, \partial_P u\right\}, \tag{A.4}$$

$$a_3 = 3xyuw + xy(h_G - h_L) + \tfrac{3}{2}xy(y-x)u^2, \tag{A.5}$$

$$a_4 = w^2 - xy\frac{u}{w}[h_G - h_L + \tfrac{1}{2}(y-x)u^2], \tag{A.6}$$

$$y_1 = 1 + \frac{\partial_h v}{w}\left\{\tfrac{3}{2}u^2 w\, \partial_v(xy) + u(h_G - h_L)\, \partial_v(xy) + \tfrac{1}{2}u^3\, \partial_v[xy(y-x)] + \frac{w}{v}a_4 + \left(\partial_v u + \frac{w}{v}\partial_w u\right)a_3\right\}, \tag{A.7}$$

$$y_2 = \rho^2\{w^2 + u^2[v(y-x)\, \partial_v x - xy]\} + 2\rho xyu\left(\partial_v u + \frac{w}{v}\partial_w u\right), \tag{A.8}$$

$$b_1 = \{[w^2 - xyu(u - 2w\, \partial_w u)]2R' - fw^2\}\frac{\rho}{R} \tag{A.9}$$

and

$$b_2 = \partial_h v\left[2\frac{R'}{R}(a_4 + a_3\, \partial_w u)\right]. \tag{A.10}$$